Optimized Multi-Ion Cavity Coupling

Stephen Begley, Markus Vogt, Gurpreet Kaur Gulati,* Hiroki Takahashi, and Matthias Keller
Department of Physics and Astronomy, University of Sussex, Brighton, BN1 9RH, United Kingdom
(Received 12 January 2016; published 31 May 2016)

Recent technological advances in cavity quantum electrodynamics (CQED) are paving the way to utilize multiple quantum emitters confined in a single optical cavity. In such systems, it is crucially important to control the quantum mechanical coupling of individual emitters to the cavity mode. In this regard, combining ion trap technologies with CQED provides a particularly promising approach due to the well-established motional control over trapped ions. Here, we experimentally demonstrate coupling of up to five trapped ions in a string to a high-finesse optical cavity. By changing the axial position and spacing of the ions in a fully deterministic manner, we systematically characterize their coupling to the cavity mode through visibility measurements of the cavity emission. In good agreement with the theoretical model, the results demonstrate that the geometrical configuration of multiple trapped ions can be manipulated to obtain optimal cavity coupling. Our system presents a new ground for exploring CQED with multiple quantum emitters, enabled by the highly controllable collective light-matter interaction.

DOI: 10.1103/PhysRevLett.116.223001

Over the past decade, techniques to localize quantum emitters inside high-finesse optical cavities have been extensively explored in the realm of cavity quantum electrodynamics (CQED) [1–5]. The CQED systems constitute one of the simplest forms of light-matter interaction, yet provide highly versatile platforms for studies in fundamental physics [6] and applications in quantum information [7]. The latter is highlighted by the recent demonstrations of quantum interfaces and elementary quantum networks with atomic systems [8–10].

So far, there have been two major strategies in atomic CQED: either employing a single atom or a large ensemble of atoms. In the latter case, only the averaged contribution from many atoms is of interest and individual atoms are not controlled [11,12]. Even though the idea to couple multiple atoms deterministically to a single optical mode dates back to the well-known Dicke model of superradiance [13], experimental efforts have started only recently [14–17]. In general, many-body interactions mediated by cavity photons in multiatom CQED give rise to far richer physics than single-atom CQED (e.g., [18,19]) and find many applications, such as quantum logic gates [20,21], nonclassical light sources [22,23], and entanglement generation schemes [24,25]. Furthermore, this system naturally fits into the quantum network architecture where each nodal station should possess a multiqubit quantum register interfaced by an optical cavity [7,26]. The major challenges in multiatom CQED lie in controlling couplings of the individual atoms to the cavity mode in its standing wave pattern while minimizing unwanted excess motion. In that regard, ion trap systems have a particular advantage in their unparalleled motional control over trapped ions. A linear string of single ions can be easily localized in the Lamb-Dicke regime; i.e., the extent of the motional wave functions of the trapped ions is smaller than the relevant optical wavelength [27]. Despite the fact that the inter-ion distances cannot be made uniform in general, for a moderate number of ions, the overall confinement can be optimized in order to couple all the ions with nearly maximal strength to the cavity mode.

In this Letter, we present an experiment to deterministically control the position and spacing of single ions trapped inside a high finesse optical cavity. In good agreement with the theory, these results demonstrate that we can achieve a simultaneous coupling of multiple ions to the cavity mode with a high degree of controllability. We also show that the presence of multiple ions can significantly enhance their localization due to their mutual Coulomb interaction.

The experimental setup is shown in Fig. 1(a). A string of $^{40}Ca^{+}$ ions is trapped in a linear Paul trap with its axis aligned to coincide with the axis of an optical cavity. This configuration enables multiple ions to be simultaneously coupled to the cavity mode. In our ion trap, the radial confinement is provided by four blade-shaped electrodes with their pointed edges arranged on a square centered around the trapping region. The distance from the trap center to the rf electrodes is 475 μm. A pair of dc end cap electrodes with a separation of 5 mm provides confinement in the axial direction. The radial secular frequency is 1.23 MHz, whereas the axial secular frequency is changed over 400–620 kHz during the experiment in order to vary the axial spacing of the ions. The stray electric fields in the trap that result in the ions' micromotion are compensated by applying correctional dc voltages onto the rf electrodes. The cavity mirrors are enclosed inside the hollow inner structure of the dc end cap electrodes [see Fig. 1(a)]. 1 mm diameter openings at the centers of the end caps allow a line

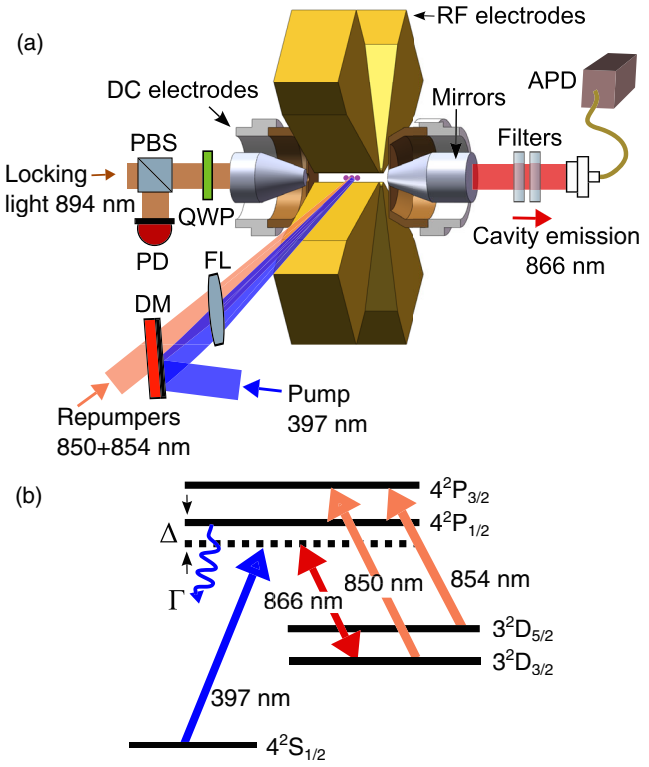

FIG. 1. (a) Experimental setup. Pump and repump laser beams are overlapped and sent obliquely to the trap axis. The cavity emission at 866 nm is detected with an avalanche photodiode (APD). A reference laser at 894 nm is used for locking the cavity frequency. A combination of filters are used to remove background light from the cavity emission. Dichroic mirror (DM), focusing lens (FL), polarization beam splitter (PBS), photodiode (PD), quarter wave plate (QWP). (b) Level scheme of $^{40}Ca^{+}$ indicating wavelengths relevant for the experiment.

of sight between the mirrors which symmetrically form an optical cavity around the trapped ions with a cavity length of 5.3 mm. Incorporating the mirrors in this way protects the trapping region from potential distortion by the dielectric surfaces of the mirrors [28]. The two cavity mirrors have transmissivities of 100 and 5 ppm at 866 nm, leading to a cavity finesse of ∼60 000 and a decay rate of $2\kappa = 2\pi \times 470$ kHz.

Figure 1(b) shows the level scheme and relevant transitions in $^{40}Ca^{+}$. The ground state $S_{1/2}$, the excited state $P_{1/2}$ and the metastable state $D_{3/2}$ form a three-level Λ system. Here, the pump beam at 397 nm on $S_{1/2} - P_{1/2}$ serves two purposes: Doppler cooling of the trapped ions and driving one arm of the cavity-assisted Raman transition. The former is accomplished by adjusting the detuning Δ of the pump beam to $\sim\Gamma/2$ on the red side of the transition. Here, $\Gamma(= 2\pi \times 22.3$ MHz) is the total decay rate of the $P_{1/2}$ state. An additional laser beam with far detuning (6.5 Γ) is used to stabilize the string of multiple ions for the measurements shown in Figs. 3 and 4. The frequency of the pump laser is stabilized through a scanning cavity lock [29] to a reference laser at 894 nm which, in turn, is locked to a cesium atomic transition. A branch of the same reference laser is used to stabilize the cavity resonance frequency with respect to the $P_{1/2} - D_{3/2}$ transition. By satisfying the Raman condition, i.e., the pump and cavity detunings being equal, a population in $S_{1/2}$ can be coherently transferred to $D_{3/2}$. This results in the emission of an 866 nm photon into the cavity mode [30]. A combination of 850 nm and 854 nm repumper lasers is employed to depopulate the metastable $D_{3/2}$ state (lifetime ≈1 s) to provide continuous cooling and cavity emission. Because of the asymmetric transmissivities of the cavity mirrors, the photon emission in the cavity is predominantly outcoupled to one direction. This directed continuous photon stream is further coupled to a single mode fiber and its rate is measured by an avalanche photodiode (APD).

We first demonstrate the coupling of a single ion to the cavity. The coupling rate g between a single ion and the cavity field varies with the local field strength at the position of the ion [31]. It is characterized by a standing wave pattern along the cavity axis (z)

$$g(z) = g_0 \cos(kz), \tag{1}$$

where $k = 2\pi/\lambda$ is the wave number of the cavity field and $2g_0$ is the vacuum Rabi frequency. With our cavity geometry, g_0 is $2\pi \times 0.9$ MHz. The variation of g along the radial direction is neglected as the cavity field varies axially on a much shorter length scale than radially. The spatial wave function of a single ion $\Psi(z)$ in a harmonic potential is described by a Gaussian distribution with a variance of

$$(\Delta z)^2 \approx \frac{2k_B T}{m\omega_{\mathrm{sec}}^2}, \tag{2}$$

where ω_{sec} is the axial secular frequency and T is the temperature of the ion. Because of this spatial fluctuation of the ion, the average cavity emission rate R_{em} is proportional to the convolution of $g(z)^2$ and $|\Psi(z)|^2$

$$R_{\mathrm{em}}(z) \propto g_0^2(1 + e^{-k^2(\Delta z)^2}\cos(2kz)). \tag{3}$$

$R_{\mathrm{em}}(z)$ is maximal (minimal) when the ion is located at an antinode (node) of the cavity field for a given Δz.

As shown in Fig. 2, this periodic dependence of $R_{\mathrm{em}}(z)$ on z is observed in the APD count, as we translate the entire cavity around a single ion while keeping the absolute position of the ion and the cavity length both constant. The contrast of this pattern reveals how well the ion is localized and is quantified by the visibility $V = (R_{\mathrm{em}}^{\mathrm{max}} - R_{\mathrm{em}}^{\mathrm{min}})/(R_{\mathrm{em}}^{\mathrm{max}} + R_{\mathrm{em}}^{\mathrm{min}})$ where $R_{\mathrm{em}}^{\mathrm{max}}$ and $R_{\mathrm{em}}^{\mathrm{min}}$ are the maximum and minimum of the observed count rate. For a single ion [31],

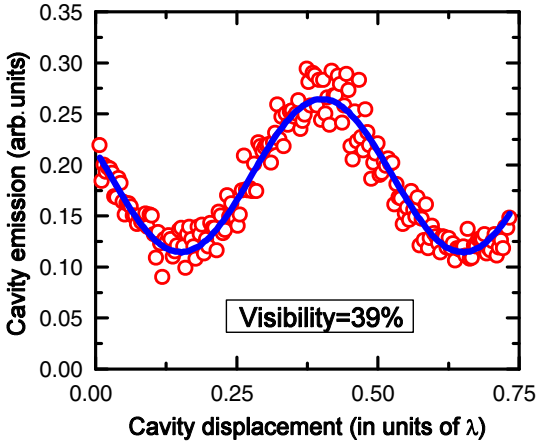

FIG. 2. Cavity emission rate R_{em} as the cavity is translated relative to the position of a single ion ($\lambda = 866$ nm). The axial secular frequency is 620 kHz. A visibility of 39% is obtained from a sinusoidal fit. This corresponds to a temperature of $\approx 1.2\ T_D$ where T_D is the Doppler temperature. Note that the far-detuned cooling beam is not used in this measurement.

$$V = e^{-k^2(\Delta z)^2}. \tag{4}$$

The visibility value of 39% shown in Fig. 2 corresponds to $\Delta z = 133$ nm and a temperature of $\approx 1.2\ T_D$ where T_D is the Doppler temperature ($= 535\ \mu$K), confirming good localization of a single ion inside the cavity. The visibility will be used as a figure of merit throughout the following analysis.

When multiple ions are weakly coupled to the cavity mode (i.e., $g_0 < \Gamma$) and repumped continuously, the total cavity emission rate is a sum in the form of $\sum_i R_{\mathrm{em}}(z_i)$ where each term $R_{\mathrm{em}}(z_i)$ represents the emission rate of each individual ion [see Eq. (3)]. The visibility for multiple ions is no longer a simple function of the localization Δz as in Eq. (4). Instead, the inter-ion spacing with respect to the cavity wavelength plays an important role [32].

Figures 3(a) and 3(b) show the visibility measurements for one and two ions as the secular frequency of the c.m. mode is varied. For each data point shown as a red circle, we performed a visibility measurement with a fixed c.m. secular frequency in the same manner as the one shown in Fig. 2 and extracted the visibility value from a sinusoidal fit. When several ions are trapped in the same potential, the ratio of the radial and axial secular frequencies determines the ions' configuration [33]. To ensure that the ions form a linear string along the trap axis, the axial trap confinement must be significantly weaker than in the radial direction. This places an upper limit on the axial c.m. secular frequencies which decreases with increasing ion number. For consistency, we have chosen the frequency range for all the measurements in Figs. 3 and 4 to be bounded by the frequency limit at which five ions remain in a linear configuration. Figure 3(c) shows the calculated inter-ion distance for two ions as a function of the c.m. secular

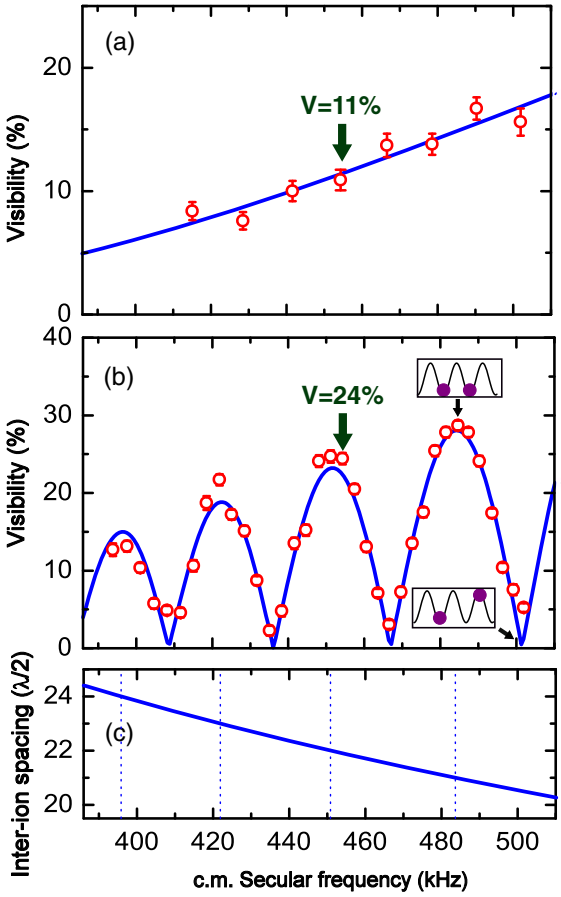

FIG. 3. Visibility measurements for (a) a single ion and (b) two ions as a function of the c.m. secular frequency. Error bars are derived from the fitting errors. The blue curves are fits based on our theoretical model (see Supplemental Material [34]). The temperatures extracted from the fits are $\sim 1.5\ T_D$ in both cases. The increase in temperature compared to Fig. 2 is due to the presence of the far detuned laser. The inset figures in (b) illustrate the relationships between the ions' positions and the spatial variation of $g^2(z)$ at a local maximum and minimum of the visibility. (c) The inter-ion spacing between two ions. The dotted vertical lines indicate the c.m. secular frequencies at which the spacing becomes an integer multiple of $\lambda/2$.

frequency. The local maxima of the visibility in Fig. 3(b) are attained when the ions are spaced by an integer multiple of $\lambda/2$, such that they can sit simultaneously at nodes or antinodes of the cavity field. At these inter-ion spacings, the two ions are coupled to the cavity mode with equal strength. In contrast, when the ions are separated by a half-integer multiple of $\lambda/2$, the total emission rate from the two ions remains constant regardless of the cavity displacement, and as a result, the visibility vanishes.

We have also observed greater values of visibility for two ions at the local maxima when compared to the measurements with a single ion at the same c.m. secular frequencies. For example, at 454 kHz in Figs. 3(a) and 3(b), the visibility value is 24% for two ions, whereas it is only 11% for a single ion. This shows that the mutual Coulomb

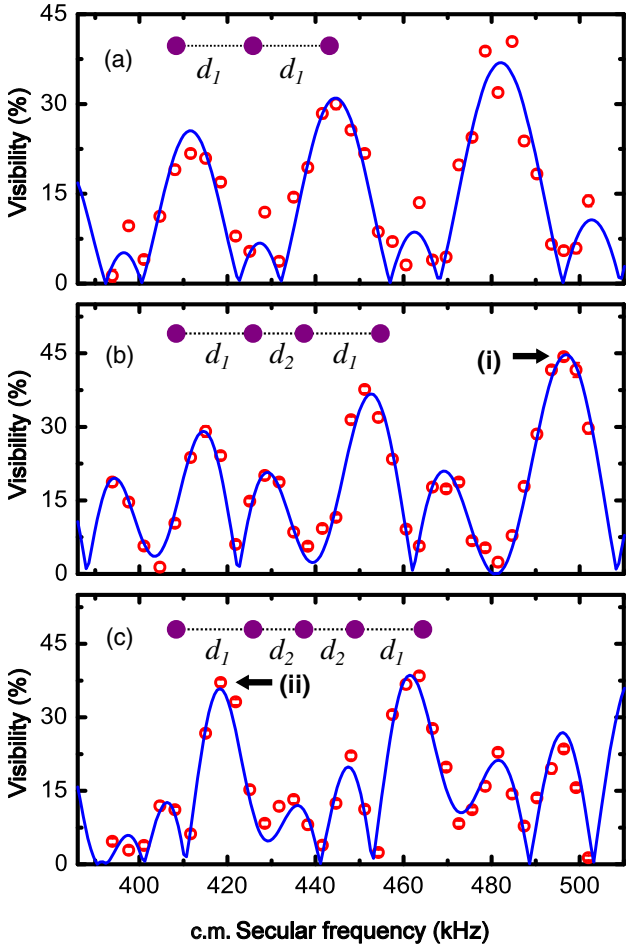

FIG. 4. Visibility measurements for (a) three, (b) four, and (c) five ion strings. The fits assume that the temperatures of all normal modes are identical. The extracted temperatures are (a) 1.56 T_D, (b) 1.57 T_D, (c) 1.72 T_D, showing a slight increase with the number of ions. The insets illustrate the configurations of ion strings. In particular, with four and five ions, the inter-ion spacing is not uniform, i.e., $d_1 \neq d_2$.

interaction between the ions contributes to an enhanced spatial confinement. In general, each ion's excursion $z_i (i = 1, \ldots, N)$ from the equilibrium position in a string of N ions can be expressed as a linear combination of normal mode amplitudes Z_i [35], i.e., $z_i = \sum_{j=1}^{N} U_{ij} Z_j$ where U_{ij} is a unitary matrix. Therefore, the spread Δz_i due to thermal motion is given by

$$\Delta z_i = \sqrt{\sum_{j=1}^{N} (U_{ij} \Delta Z_j)^2}, \qquad i = 1, \ldots, N. \tag{5}$$

For two ions, this becomes $\Delta z_{1,2} = \sqrt{[(\Delta Z_{\text{c.m.}})^2 + (\Delta Z_{\text{STR}})^2]/2}$ where $\Delta Z_{\text{c.m.}}$ and ΔZ_{STR} are the amplitude fluctuations of the c.m. and stretch (STR) mode, respectively. Both $\Delta Z_{\text{c.m.}}$ and ΔZ_{STR} obey Eq. (2), and since the stretch mode has a higher eigenfrequency than the c.m. mode ($\omega_{\text{STR}} = \sqrt{3}\omega_{\text{c.m.}}$), they satisfy $\Delta Z_{\text{STR}} < \Delta Z_{\text{c.m.}}$ if both modes are at the same temperature. This results in $\Delta z_{1,2} < \Delta Z_{\text{c.m.}}$, which, in turn, means that $\Delta z_{1,2}$ is smaller than Δz for a single ion. This argument can be extended to N ions, and it can be shown that $\Delta z_i < \Delta Z_{\text{c.m.}} (i = 1, \ldots, N)$ is satisfied, in general (see Supplemental Material [34]). Therefore, it is possible to achieve a higher degree of ion localization and, hence, higher visibility values for a larger number of ions if the temperatures of the high-order modes are comparable to the c.m. mode temperature.

Figure 4 shows visibility measurements with three, four, and five ions performed in the same frequency range as Fig. 3. Our theoretical model (shown in blue curves) fits to all the data points very well. These results demonstrate that, despite more complex variations in V, it is possible to achieve simultaneous cavity coupling of three to five ions with a visibility of up to 40%. A closer look at individual data points reveals more details about the ions' geometrical configuration. As is the case with two ions, the major local maxima in the three ions' visibility plot correspond to the ion spacing d_1 being an integer multiple of $\lambda/2$. Namely, $d_1 = 20$, 19, and 18 in units of $\lambda/2$ at 411, 444, and 482 kHz, respectively. However, for more than three ions, the inter-ion spacing is no longer uniform [35]. In the cases of four and five ions, there are two unequal distances d_1 and d_2 between the ions as shown in Fig. 4. Nevertheless, these inter-ion distances can be optimized to yield the best possible cavity coupling in the given frequency range. At the data points denoted as (i) and (ii) in Figs. 4(b) and 4(c), the following parameters are extracted from the theoretical fits: (i) $d_1 = 16.1$, $d_2 = 14.9$ and (ii) $d_1 = 16.9$, $d_2 = 15.1$ in units of $\lambda/2$. In order to evaluate the inhomogeneities amongst the ions' cavity coupling strengths at these points, we define the normalized average coupling strength as $\tilde{g} = 1/(g_0 N) \sum_{i=1}^{N} |g(z_i^0)|$ where $g(z_i^0)$ is given by Eq. (1) evaluated at each ion's equilibrium position z_i^0, and N is the total number of ions. At optimized cavity displacements, we obtain $\tilde{g} = 0.988$ and 0.983 for the points (i) and (ii), respectively, from the extracted d_1 and d_2. These results show that, despite the unequal inter-ion spacing with four and five ions, we are able to couple all the ions to the cavity mode with nearly maximal strength with errors of less than 2%.

This Letter has explored a previously uncharted territory of coupling up to five trapped ions to a single cavity mode in a fully deterministic way. We have thoroughly characterized the collective coupling of multiple ions through visibility measurements of the detected cavity emission. In good agreement with the theoretical model, the results confirm our capability for controlling the geometrical configuration of ions to optimize the cavity coupling. An enhanced localization due to the mutual Coulomb interaction between multiple ions has also been observed. Currently, our system is in the intermediate coupling

regime with a collective cooperativity of $Ng_0^2/(\kappa\Gamma) = 0.78$ with five ions ($N = 5$). Despite not being in the strong coupling regime, this system may be used to observe multi-ion collective effects, such as super- or subradiance, upon postselection of events [17] and is generally suitable for heralded schemes for entanglement generation [36]. Improvement on the current cavity finesse is possible with state-of-the-art mirror coatings [37], leading to a potential enhancement of the cooperativity by a factor of 10–20. These results and prospects make our axial-trap-cavity design an extremely attractive candidate for implementing a few-qubit CQED system for studies in many-body entanglement and applications in optical quantum information processing networks.

We gratefully acknowledge support from the EPSRC (Grants No. EP/M013243/1 and No. EP/J003670/1).

*Gurpreet.Kaur@sussex.ac.uk

[1] R. Miller, T. E. Northup, K. M. Birnbaum, A. Boca, A. D. Boozer, and H. J. Kimble, J. Phys. B **38**, S551 (2005).
[2] M. Keller, B. Lange, K. Hayasaka, W. Lange, and H. Walther, Nature (London) **431**, 1075 (2004).
[3] T. Yoshie, A. Scherer, J. Hendrickson, G. Khitrova, H. M. Gibbs, G. Rupper, C. Ell, O. B. Shchekin, and D. G. Deppe, Nature (London) **432**, 200 (2004).
[4] Y. Colombe, T. Steinmetz, G. Dubois, F. Linke, D. Hunger, and J. Reichel, Nature (London) **450**, 272 (2007).
[5] A. Faraon, C. Santori, Z. Huang, V. M. Acosta, and R. G. Beausoleil, Phys. Rev. Lett. **109**, 033604 (2012).
[6] J. Raimond, M. Brune, and S. Haroche, Rev. Mod. Phys. **73**, 565 (2001).
[7] H. J. Kimble, Nature (London) **453**, 1023 (2008).
[8] T. Wilk, S. C. Webster, A. Kuhn, and G. Rempe, Science **317**, 488 (2007).
[9] S. Ritter, C. Nölleke, C. Hahn, A. Reiserer, A. Neuzner, M. Uphoff, M. Mücke, E. Figueroa, J. Bochmann, and G. Rempe, Nature (London) **484**, 195 (2012).
[10] A. Stute, B. Casabone, B. Brandstätter, K. Friebe, T. E. Northup, and R. Blatt, Nat. Photonics **7**, 219 (2013).
[11] P. F. Herskind, A. Dantan, J. P. Marler, M. Albert, and M. Drewsen, Nat. Phys. **5**, 494 (2009).
[12] R. McConnell, H. Zhang, J. Hu, S. Ćuk, and V. Vuletić, Nature (London) **519**, 439 (2015).
[13] R. Dicke, Phys. Rev. **93**, 99 (1954).
[14] B. Casabone, A. Stute, K. Friebe, B. Brandstätter, K. Schüppert, R. Blatt, and T. E. Northup, Phys. Rev. Lett. **111**, 100505 (2013).
[15] M. Cetina, A. Bylinskii, L. Karpa, D. Gangloff, K. M. Beck, Y. Ge, M. Scholz, A. T. Grier, I. Chuang, and V. Vuletić, New J. Phys. **15**, 053001 (2013).
[16] R. Reimann, W. Alt, T. Kampschulte, T. Macha, L. Ratschbacher, N. Thau, S. Yoon, and D. Meschede, Phys. Rev. Lett. **114**, 023601 (2015).
[17] B. Casabone, K. Friebe, B. Brandstätter, K. Schüppert, R. Blatt, and T. E. Northup, Phys. Rev. Lett. **114**, 023602 (2015).
[18] S. Morrison and A. S. Parkins, Phys. Rev. Lett. **100**, 040403 (2008).
[19] S. Gopalakrishnan, B. L. Lev, and P. M. Goldbart, Phys. Rev. Lett. **107**, 277201 (2011).
[20] T. Pellizzari, S. A. Gardiner, J. I. Cirac, and P. Zoller, Phys. Rev. Lett. **75**, 3788 (1995).
[21] S.-B. Zheng, Phys. Rev. A **70**, 052320 (2004).
[22] S. Fernández-Vidal, S. Zippilli, and G. Morigi, Phys. Rev. A **76**, 053829 (2007).
[23] H. Habibian, S. Zippilli, and G. Morigi, Phys. Rev. A **84**, 033829 (2011).
[24] A. González-Tudela and D. Porras, Phys. Rev. Lett. **110**, 080502 (2013).
[25] E. G. Dalla Torre, J. Otterbach, E. Demler, V. Vuletic, and M. D. Lukin, Phys. Rev. Lett. **110**, 120402 (2013).
[26] S. J. van Enk, J. I. Cirac, and P. Zoller, Phys. Rev. Lett. **78**, 4293 (1997).
[27] D. Leibfried, R. Blatt, C. Monroe, and D. Wineland, Rev. Mod. Phys. **75**, 281 (2003).
[28] M. Harlander, M. Brownnutt, W. Hänsel, and R. Blatt, New J. Phys. **12**, 093035 (2010).
[29] N. Seymour-Smith, P. Blythe, M. Keller, and W. Lange, Rev. Sci. Instrum. **81**, 075109 (2010).
[30] M. Keller, B. Lange, K. Hayasaka, W. Lange, and H. Walther, Eur. Phys. J. D **32**, 161 (2005).
[31] G. Guthoehrlein, M. Keller, K. Hayasaka, W. Lange, and H. Walther, Nature (London) **414**, 49 (2001).
[32] A. Bylinskii, D. Gangloff, and V. Vuletić, Science **348**, 1115 (2015).
[33] D. Kielpinski, B. E. King, C. J. Myatt, C. A. Sackett, Q. A. Turchette, W. M. Itano, C. Monroe, D. J. Wineland, and W. H. Zurek, Phys. Rev. A **61**, 032310 (2000).
[34] See Supplemental Material at http://link.aps.org/supplemental/10.1103/PhysRevLett.116.223001 for the description of a theoretical model to fit visibility measurements and explanation of enhanced localization in a multi-ion string.
[35] D. F. V. James, Appl. Phys. B **66**, 181 (1998).
[36] L.-M. Duan and H. J. Kimble, Phys. Rev. Lett. **90**, 253601 (2003).
[37] G. Rempe, R. J. Thompson, H. J. Kimble, and R. Lalezari, Opt. Lett. **17**, 363 (1992).